Contribution from the Department of Chemistry,
University of Houston, Houston, Texas 77004

Counterion and Solvent Effects on the Electrode Reactions of Manganese Porphyrins

S. L. KELLY and K. M. KADISH*

Received February 23, 1982

A systematic study of the interacting effects of solvent and axially coordinated monovalent anions on the electrode reactions of manganese porphyrins is presented. Six different anions were coordinated to (5,10,15,20-tetraphenylporphinato)-manganese(III), and their respective redox reactions were investigated in 12 nonaqueous solvents. Potential shifts of the metal-centered reaction with changes in counterion were related to the degree of Mn(III)–counterion interaction. Potential shifts of the various redox reactions with changes in solvent were related to the solvent parameters of donor number, acceptor number, and dielectric constant. Studies in mixed-solvent systems revealed a finely balanced competition between counterion and strongly donating solvents for axial coordination to Mn(III). Formation constants for axial ligation of Me_2SO, pyridine, and imidazole to Mn(III) and Mn(II) are presented and discussed.

Introduction

In the last 20 years extensive measurements of Mn(III)/Mn(II) redox potentials[1-11] and spectroscopic characterization[6-8,12-17] of Mn(III) and Mn(II) under varying solution conditions have been published. In aqueous and nonaqueous media, Mn(III) porphyrins may be electrochemically reduced in a single electron transfer step to yield a porphyrin containing a Mn(II) central ion. In nonaqueous media, the anion radical and dianion of Mn(II) may be formed.[18,19] The Mn(III) complex may also be oxidized in nonaqueous media to yield Mn(III) cation radicals and dications.[18,19] The potentials of these reactions are dependent on the solvent, counterion on Mn(III), pK_a, and/or steric effects of any bound ligands, as well as the porphyrin ring basicity.

In 1970, Boucher and Garber[6] reported polarographic half-wave potentials in acetonitrile and DMF for the reduction of seven different manganese porphyrins containing nine different counterions. Aceonitrile was selected because it is a good polarographic solvent while DMF was used so that comparisons could be made with prior literature. On the basis of their results it was concluded that the polarographic half-wave potentials for both Mn(III) and Mn(II) reduction depended upon the basicity of the porphyrin ring and that $E_{1/2}$ for Mn(III)/Mn(II) was also dependent upon the strength of the counterion bound to Mn(III). Potentials for the second (and third) reduction were found to be independent of the starting anion on Mn(III).

The most extensive data relating Mn(III) counterion to half-wave potentials were presented by Boucher and Garber[6] for complexes of (P)MnX(H_2O) where P was protoporphyrin IX dimethyl ester or etioporphyrin I. Complexation of the starting material with weak counterions such as I^- or Br^- gave reductions with the most positive values of $E_{1/2}$ in acetonitrile while strong counterions such as F^- or $C_2H_3O_2^-$ gave the most negative values. It was also pointed out that the order of half-wave potentials followed the electronegativity of the donor atom and that, of the anions investigated, F^- formed the strongest complex with Mn(III). The conclusion reached was that the stronger the halide–manganese bond the more Mn(III) is stabilized with respect to Mn(II). No information, however, was presented regarding the solvent interaction with Mn(III) or Mn(II). Because of the fact that only two strongly bonding solvents were utilized in this study, it was impossible to determine from the published data what would be the effect of solvent in directing the electron-transfer reactions or how the influence of bound counterions might be modified by changing the nature of the nonaqueous solvent. This point had been recently considered for the reactions of synthetic iron porphyrin complexes where it had been shown that potentials for the first and second reduction of (TPP)FeX could vary by up to 720 and 480 mV, respectively, depending on the nature of the solvent system,[20] the nature of X^-, and possibly spin state. Iron porphyrins have been characterized as having three different types of spin state. In contrast, manganese porphyrins are invariably high spin when complexes with anions or neutral nitrogenous bases. Thus, the variable of spin-state change is eliminated. This fact, combined with earlier implications of Mn(II) porphyrin binding by anions,[11] indicated that a systematic and complex study of the interacting effects of solvent and counterion on Mn porphyrin redox reactions was needed.

This paper presents the results of such a study. Six different anions were coordinated to $[(TPP)Mn^{III}]^+$, and their respective redox reactions were investigated in twelve different nonaqueous solvents. Potential shifts with changes in solvent and counterion were directly related to solvent donicity, changes in dielectric constant of the solvent, changes in spectra, and changes in conductivity of the starting solution. On the basis of these data, a clear picture of the interdependence of solvent–counterion coordination to the Mn(III) and Mn(II) center emerges. In addition, several mechanisms of oxidation/reduction are presented and binding constants calculated for addition of pyridine and Me_2SO to the Mn(III) and Mn(II) central ion in a nonbonding solvent.

Experimental Section

Methods. Cyclic voltammetric experiments were made on a PAR Model 174A polarographic analyzer utilizing the three-electrode configuration of a Pt-button working electrode, a Pt-wire counter-electrode, and a commercially available saturated calomel electrode (SCE) as a reference electrode. An Omnigraphic 2000 X-Y recorder

(1) P. A. Loach and M. Calvin, *Biochemistry*, **2**, 361 (1963).
(2) P. A. Loach and M. Calvin, *Nature (London)*, **202**, 345 (1964).
(3) M. Calvin, *Rev. Pure Appl. Chem.*, **15**, 1 (1965).
(4) D. G. Davis and J. G. Montalvo, Jr., *Anal. Lett.*, **1**, 641 (1968).
(5) D. G. Davis and J. G. Montalvo, Jr., *Anal. Chem.*, **41**, 1195 (1965).
(6) L. J. Boucher and H. K. Garbor, *Inorg. Chem.*, **9**, 2644 (1970).
(7) L. J. Boucher, *Coord. Chem. Rev.*, **7**, 289 (1972).
(8) L. J. Boucher, *Ann. N.Y. Acad. Sci.*, **206**, 409 (1973).
(9) K. M. Kadish and M. M. Morrison, *Bioelectrochem. Bioenerg.*, **3**, 480 (1977).
(10) K. M. Kadish, M. Sweetland, and J. S. Cheng, *Inorg. Chem.*, **17**, 2795 (1978).
(11) K. M. Kadish and S. Kelly, *Inorg. Chem.*, **18**, 2968 (1979).
(12) L. J. Boucher, *J. Am. Chem. Soc.*, **90**, 6640 (1968).
(13) L. J. Boucher, *J. Am. Chem. Soc.*, **92**, 2725 (1970).
(14) G. N. LaMar and F. A. Walker, *J. Am. Chem. Soc.*, **97**, 5103 (1975).
(15) R. D. Jones, D. A. Summerville, and F. Basolo, *J. Am. Chem. Soc.*, **95**, 4416 (1978).
(16) B. M. Hoffman, C. J. Weschler, and F. Basolo, *J. Am. Chem. Soc.*, **98**, 5473 (1976).
(17) B. M. Hoffman, T. Szymanski, T. G. Brown, and F. Basolo, *J. Am. Chem. Soc.*, **100**, 7253 (1978).
(18) R. H. Felton in "The Porphyrins", Vol. 3, D. Dolphin, Ed., Academic Press, New York, 1978.
(19) J. H. Fuhrhop in "Porphyrins and Metalloporphyrins", K. Smith, Ed., Elsevier, New York, 1978.
(20) L. A. Bottomley and K. M. Kadish, *Inorg. Chem.*, **20**, 1348 (1981).

0020-1669/82/1321-3631$01.25/0

was used to record the current–voltage output. Half-wave potentials were measured as the average of the cathodic and anodic peak potentials, $(E_{pa} + E_{pc})/2$.

Coulometric experiments were performed with a PAR Model 173 potentiostat/galvanostat and Model 179 digital coulometer in conjunction with a Model 178 electrometer probe. A three-electrode configuration was used, consisting of a Pt-wire mesh working electrode, Pt-wire counterelectrode separated from the main solution by a glass frit, and an SCE as the reference electrode. The coulometric cell contained a quartz window (2.0-mm path length) at the bottom, allowing the electronic absorption spectra of the reactant and product be taken in situ. The configuration of the cell was such that bubbling of N_2 gas through the cell would allow all portions of the bulk solution to be reduced at the working electrode. A Tracor Northern 1710 holographic optical spectrometer/multichannel analyzer was used to obtain time-resolved spectra. Spectra result from the signal averaging of 100 sequential 5-ms spectral acquisitions. Each acquisition represents a single spectrum from 350 to 750 nm simultaneously recorded by a silicon diode array detector with a resolution of 1.2 nm/channel.

For all electrochemical experiments, the reference electrode was separated from the bulk of solution by a fritted bridge filled with solvent and supporting electrolyte. The solution in the bridge was changed periodically to prevent aqueous contamination of the cell solution by the reference electrode. Deaeration of all solutions was accomplished by passing a constant stream of high-purity nitrogen or argon through the solution for 10 min and maintaining a blanket of inert gas over the solution during the experiment. The inert gas was saturated with solvent prior to entering the cell.

A Model 31 YSI conductivity bridge was used to measure solution conductances. Measurements were taken in a Metrohm AG Herisau Model EA 655 cell (cell constant 0.092 cm^{-1}), which was immersed in a temperature bath of 25.00 ± 0.05 °C. All values are reported as molar conductances.

Calculation of Formation Constants from Spectrophotometric Data. Solutions for spectrophotometric measurements were prepared in 1,2-dichloroethane, $EtCl_2$, containing 0.1 M tetrabutylammonium perchlorate, TBAP, and 1.05×10^{-5} M (TPP)$MnClO_4$, with ligand to porphyrin ratios ranging from 0:1 to 4000:1. The ligands reported are pyridine, Me_2SO, and imidazole. Absorption spectra were obtained on a Cary 14 spectrophotometer at 25.00 ± 0.5 °C. As the spectra obtained were not simplified by the presence of isobestic points, the data were analyzed by SQUAD, a sophisticated computer program that tests various equilibrium models against a spectral data set and refines the initial estimates of stability constants for the model under consideration.[21,22] The application of SQUAD to the data allowed detection of mono and bis complexes of $[(TPP)Mn^{III}]^+$ for each of the three ligands and determination of the associated equilibrium constants. An application of SQUAD toward the determination of stability constants of Mg porphyrins has recently appeared.[23]

Materials. The supporting electrolytes were tetrabutylammonium salts of perchlorate (TBAP), bromide ((TBA)Br) and chloride ((TBA)Cl). These were obtained from Eastman Chemicals or Fluka and were dried in vacuo prior to use. TBAP was first recrystallized from ethanol/ethyl ether and then dried in vacuo at 40 °C.

Twelve different nonaqueous, aprotic solvents were used throughout this study. Nitromethane, $MeNO_2$ (Baker Chemical), dimethyl sulfoxide, Me_2SO (Eastman Chemical), dimethyl acetamide, DMA (Fisher Scientific), and benzonitrile, PhCN (Aldrich Chemical), were received as reagent grade from the manufacturer and were dried over 4-Å molecular sieves prior to use. Dichloroethane was purchased from Mallinckrodt. Prior to use, portions were extracted with equal volumes of concentrated H_2SO_4, distilled H_2O, and a 5% KOH solution. The extract was then distilled from P_2O_5 and stored in the dark over activated 4-Å molecular sieves. Methylene chloride, CH_2Cl_2, obtained from Fisher Scientific as technical grade was treated in a similar fashion. Butyronitrile, PrCN, was obtained from Aldrich Chemical and was purified by the method of VanDuyne and Reilly.[24] Matheson Coleman and Bell was the supplier for acetonitrile, MeCN, and acetone, $(CH_3)_2CO$, which were dried over 4-Å molecular sieves after distillation. Tetrahydrofuran, THF, was also supplied by Matheson Coleman and Bell. This solvent was distilled under N_2 over Na immediately prior to use. Dimethylformamide, DMF, was treated with 4-Å molecular sieves after purchase from Baker Chemicals. When DMF was obtained from Eastman Chemical, it was first shaken with KOH, distilled from CaO under N_2, and stored over 4-Å molecular sieves before use. Pyridine, py, was distilled over KOH.

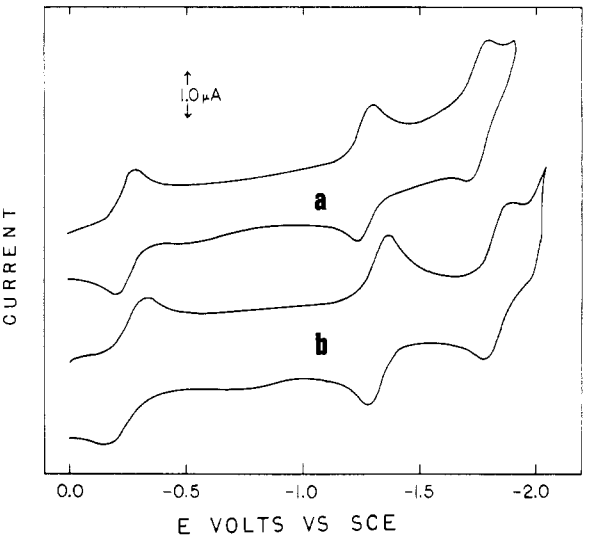

Figure 1. Cyclic voltammograms of (TPP)$MnClO_4$ in (a) Me_2SO and (b) pyridine solutions containing 0.1 M TBAP (scan rate 200 mV/s).

(TPP)MnCl was synthesized by the method of Adler,[25] using chlorin-free H_2TPP and $MnCl_2 \cdot 4H_2O$. (TPP)MnX (X = I^-, SCN^-, Br^-, and N_3^-) were synthesized by a method adopted from Boucher.[26] Typically, 200 mg of (TPP)MnOAc (synthesized or obtained from Strem Chemical) was dissolved in a minimum amount of MeOH (~30 mL) and the solution was poured into an equal volume of aqueous solution saturated with the appropriate sodium or potassium salt of X^-. The resulting green precipitate was collected on a filter and washed with a large volume of water. This procedure was repeated twice to ensure complete displacement of the acetate. The final product was dried in vacuo at 100 °C for 8 h and recrystallized from toluene/hexane. Comparison with the reported spectra of (TPP)MnX[26] showed good agreement. However, attempts to produce the fluoride salt from saturated NaF solutions produced a complex insoluble in a wide range of solvents. Attempts to synthesize the fluoride salt from H_2TPP and MnF_2 had little success, with the majority of the free-base porphyrin remaining unreacted. Except for the case of the fluoride salts, synthesis of (TPP)MnX from H_2TPP and the appropriate $MnX_2 \cdot nH_2O$ via Adler's method produced compounds having spectroscopic and electrochemical properties identical with those derived from (TPP)MnOAc.

Synthesis of (TPP)$MnClO_4$ was achieved by gentle reflux of equimolar amounts of (TPP)MnCl and $AgClO_4$ in THF using Schlenk apparatus, according to the method of Landrum et al.[27] It is noted in ref 27 that no shock sensitivity is observed, but precautions should be taken with quantities greater than 50 mg. IR spectra (KBr disk) and UV–visible spectra in THF and toluene were in good agreement with published results.

Results and Discussion

Figure 1 illustrates typical cyclic voltammograms of (TPP)$MnClO_4$ obtained in Me_2SO and in pyridine. In both solvents three well-defined reduction waves are obtained. The first at −0.25 and −0.23 V, respectively, corresponds to the reaction

$$Mn(III) \overset{e^-}{\rightleftharpoons} Mn(II)$$

(21) D. J. Leggett and W. A. McBryde, *Anal. Chem.*, **47**, 1065 (1975).
(22) D. J. Leggett, *Anal. Chem.*, **49**, 276 (1977).
(23) K. M. Kadish and L. R. Shiue, *Inorg. Chem.*, **21**, 1112 (1982).
(24) R. P. VanDuyne and C. N. Reilley, *Anal. Chem.*, **44**, 142 (1972).
(25) A. D. Adler, F. R. Longo, F. Kampas, and J. Kim, *J. Inorg. Nucl. Chem.*, **32**, 2443 (1970).
(26) R. R. Gaughan, D. F. Shriver, and L. J. Boucher, *Proc. Natl. Acad. Sci., U.S.A.*, **72**, 433 (1975).
(27) J. T. Landrum, K. Hatano, W. R. Scheidt, and C. A. Reed, *J. Am. Chem. Soc.*, **102**, 6729 (1980).

Table I. Half-Wave Potentials (V) vs. SCE of the Mn(III)/Mn(II) Redox Couple for (TPP)MnX in Selected Solvents

			counterion, X					
solvent	DN	dielec const	ClO_4^-	I^-	SCN^-	Br^-	Cl^-	N_3^-
$MeCl_2$	0.0	8.9	−0.16	−0.24	−0.25	−0.26	−0.29	−0.34
$EtCl_2$	0.0	10.7	−0.17	−0.23	−0.23	−0.25	−0.26	−0.31
CH_3NO_2	2.7	35.9	−0.22	−0.24	−0.26	−0.28	−0.29	−0.38
PhCN	11.9	25.2	−0.14	−0.16	−0.23	−0.24	−0.27	−0.30
CH_3CN	14.1	37.5	−0.19	−0.19	−0.20	−0.20	−0.23	−0.29
PrCN	16.6	20.3	−0.13	−0.14	−0.17	−0.18	−0.22	−0.26
$(CH_3)_2CO$	17.0	20.7	−0.09	−0.07	−0.07	−0.09	−0.14	−0.17
THF	20.0	7.6	−0.12	−0.12	−0.18	−0.16	−0.23	−0.31
DMF	26.6	38.3	−0.19	−0.19	−0.19	−0.20	−0.20	−0.20
DMA	27.8	37.8	−0.12	−0.12	−0.11	−0.11	−0.11	−0.12
Me_2SO	29.8	46.4	−0.25	−0.25	−0.25	−0.25	−0.25	−0.25
py	33.1	12.0	−0.23	−0.23	−0.24	−0.23	−0.24	−0.25

Table II. Equivalent Conductances (mhos/(cm equiv)) of (TPP)MnX in Selected Solvents

				counterion, X			
solvent	DN	dielec const	TBAP	ClO_4^-	I^-	Cl^-	N_3^-
$MeCl_2$	0.0	8.9	40.4	4.4	1.6	0.7	1.8
$EtCl_2$	0.0	10.7	59.2	1.7	1.2	0.2	1.1
CH_3NO_2	2.7	35.9	191.2	142.9	21.5	11.2	16.0
PhCN	11.9	25.2	76.8	72.5	18.8	12.6	7.5
MeCN	14.1	37.5	266.7	211.0	172.4	4.9	2.3
PrCN	16.6	20.3	137.8	127.7	35.0	~0.0	~0.0
$(CH_3)_2CO$	17.0	20.7	277.7	198.5	83.5	3.3	0.2
THF	20.0	7.6	8.9	50.4	6.2	0.7	0.6
DMF	26.6	38.3	203.3	124.5	135.9	60.1	23.2
DMA	27.8	37.8	127.6	91.2	102.5	54.3	20.5
Me_2SO	29.8	46.4	75.3	62.4	66.9	68.6	43.7
py	33.1	12.0	94.1	96.0	98.1	16.3	5.9

The second reduction occurs at −1.28 V in Me_2SO and −1.31 V in pyridine and can be assigned as formation of the anion radical. The third reduction process, which is formation of the dianion, occurs at −1.77 V in Me_2SO and −1.82 V in pyridine.

The observed potentials for all reactions in Figure 1 are in general agreement with those reported in the literature for reduction of (TPP)MnCl in Me_2SO[9,10] and pyridine.[11] Reversible half-wave potentials for the first reduction were reported as occurring at −0.23 V in both solvents while in CH_2Cl_2 and reported value in the literature was −0.30 V.[11] This second value was measured at a Pt electrode and is vs. SLCE, but both are uncorrected for liquid-junction potential.

Redox Potentials of Mn(III)/Mn(II). Half-wave potentials were measured for the first reduction of six (TPP)MnX complexes in twelve nonaqueous solvents, and are reported in Table I vs. SCE. As seen from this table in the nonbonding solvent $MeCl_2$, the reduction of (TPP)MnX becomes more difficult by 180 mV as X is varied from ClO_4^- to N_3^-. The Mn(III)–counterion binding strength increases in the order $ClO_4^- < I^- < SCN^- \simeq Br^- < Cl^- < N_3^-$, and this is reflected in the increasing stabilization of Mn(III) over Mn(II) as one progresses along the series. Similar results are obtained in $EtCl_2$, $MeNO_2$, CH_3CN, PhCN, PrCN, $(CH_3)_2CO$, and THF.

The effect of counterion upon the M(III)/M(II) reaction is considerably less for (TPP)MnX than was observed for (TPP)FeX.[20] A comparison of the two metalloporphyrins shows that the Fe(III)/Fe(II) couple is shifted by 640 mV in $MeCl_2$ by varying the counterion from ClO_4^- to N_3^-,[20] while the Mn(III)/Mn(II) couple shifted by only 180 mV. Also, the crystal structures of (TPP)MnCl[28] and (TPP)FeCl[29] show that the Mn–Cl bond distance is nearly equal to the sum of the ionic radii, while the Fe–Cl bond is considerably shorter, reflecting the strong axial interaction characteristic of Fe porphyrins. This behavior again reflects the relative indifference of Mn(III) toward axial coordination, caused by the strong interaction with the porphyrin ring.

The equivalent conductance of (TPP)MnX in selected solvents is shown in Table II. Also included in this table is the equivalent conductance of TBAP, which is assumed to be completely dissociated in solution. As seen from the data, the equivalent conductance of (TPP)$MnClO_4$ varies substantially as a function of solvent, but in strongly coordinating solvents the values are similar between TBAP and (TPP)$MnClO_4$. This similarity in equivalent conductances betwen TBAP and (TPP)$MnClO_4$ in solvents of higher dielectric constants than 10.7 suggests the complete dissociation of ClO_4^- from (TPP)$MnClO_4$ according to eq 1 or 2.

$$(TPP)MnClO_4 \rightleftarrows [(TPP)Mn]^+ + ClO_4^- \quad (1)$$

$$(TPP)MnClO_4 + xS \rightleftarrows (TPP)Mn(S)_x^+ + ClO_4^- \quad (2)$$

As seen in Table II, however, the behavior of (TPP)MnX, where X = I^-, Cl^-, or N_3^-, is dependent upon both the nature of the counterion and the solvent. In nonbonding solvents, where X = I^-, Cl^-, or N_3^-, (TPP)MnX behaves essentially as a nonelectrolyte. In the more strongly bonding solvents, the extent of dissociation decreases along the order $I^- > Cl^- > N_3^-$. This trend reflects the competition between counterion and solvent for the fifth or sixth axial position of Mn(III) and agrees with the relative binding strengths of the counterions.

Ionic strength also plays a role in determining the extent of counterion dissociation as shown by eq 1 and 2. This can be demonstrated from visible spectra comparison. For example, spectra of pyridine solutions of (TPP)MnX in the absence of supporting electrolyte are identical when X = ClO_4^-, I^-, or Br^- and correspond to the spectrum of (TPP)$Mn(Py)_2^+$. This is shown in Figure 2, which illustrates the spectrum of (TPP)Mn(py) electrochemically generated from (TPP)Mn$(py)_2^+$. The spectrum of (TPP)MnCl does not differ greatly from these, but (TPP)MnN_3 solutions show peak maxima as well as peak intensity ratios different from those of the other

(28) A. Tulinsky and B. M. L. Chen, *J. Am. Chem. Soc.*, **99**, 3646 (1977).
(29) J. L. Heard, G. H. Cohen, M. D. Glick, *J. Am. Chem. Soc.*, **89**, 1992 (1967).

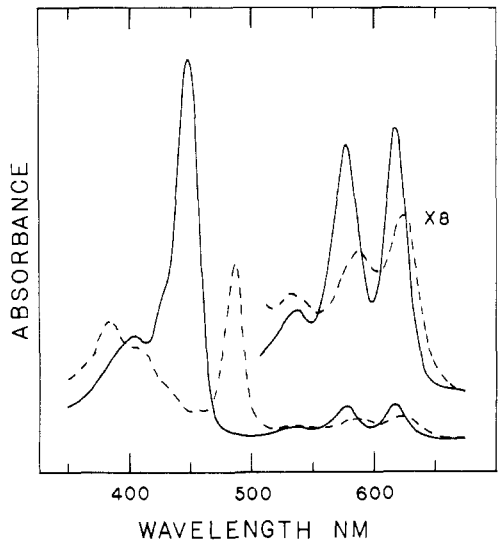

Figure 2. Visible spectra of $[(TPP)Mn(py)_2]^+$ in pyridine solution containing 0.1 M TBAP (dotted lines) and the electrochemically generated (TPP)Mn(py) (solid lines).

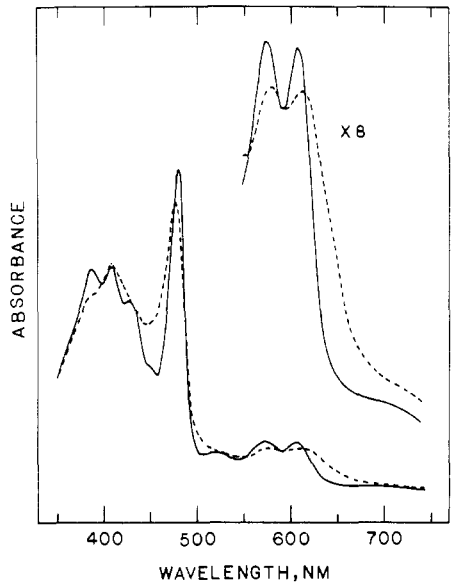

Figure 3. Visible spectra of $(TPP)MnN_3$ in pyridine solution before addition of supporting electrolyte (dotted lines) and after addition of 0.1 M TBAP to solution (solid lines).

solutions. Addition of 0.1 M TBAP to (TPP)MnCl and $(TPP)MnN_3$ solutions produced a change of spectra such that they were nearly identical with those for solutions of (TPP)MnX with weaker counterions in neat pyridine. This is shown in Figure 3 for the case of $(TPP)MnN_3$, where the change is most dramatic. Thus, from these data an increase in ionic strength is seen to favor dissociation of the counterion.

The fact that half-wave potentials for reduction of (TPP)MnX are invariant in DMA, DMF, Me_2SO, and pyridine (Table I) but shift with the counterion in other less strongly bonding solvents strongly suggests that associated (TPP)MnX rather than dissociated $[(TPP)Mn]^+$ is the electrochemical reactant in weakly bonding solvents. This conclusion also follows from the conductivity of (TPP)MnX in each solvent (Table II) although care must be taken in extrapolating from conductivity results obtained in the absence of supporting electrolyte to electrochemical measurements made in the presence of 0.1 M TBAP.

Correlations of $E_{1/2}$ for Mn(III)/Mn(II) with Solvent Properties. Correlations between half-wave potentials for a given complex and the bonding/coordinating properties of the

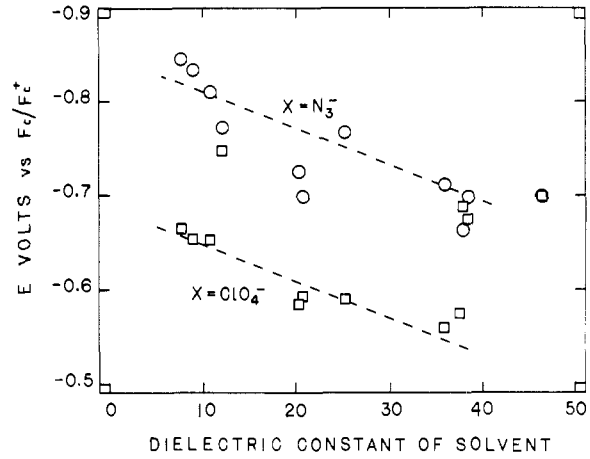

Figure 4. Plot of half-wave potentials for the metal-centered reactions of $(TPP)MnClO_4$ (□) and $(TPP)MnN_3$ (○) in 12 nonaqueous solvents vs. the dielectric constant of that solvent.

solvent have often involved plots of $E_{1/2}$ vs. the solvent donor number, DN, or solvent acceptor number, AN.[30] Generally for metalloporphyrin electrode reactions of the type M(III)/M(II), where M = Fe, Co, or Cr, half-wave potentials have been linearly related to the solvent donor number.[20,31]

A stabilization of M(III) over M(II) with increasing donor number suggests that solvent bonding is a dominant factor in the metal-centered reactions. While $(TPP)MnClO_4$ has been shown to experience such a stabilization, the effect on $(TPP)MnClO_4$ potentials is minimal compared to that of the analogous $(TPP)FeClO_4$ and (TPP)Co complexes.[31] This would imply either a weak bonding to Mn(III) by solvent molecules or an almost equal magnitude of bonding constants for Mn(III) and Mn(II). As will be discussed later in the paper, the latter choice is the more likely.

Plots of $E_{1/2}$ vs. DN were not linear for all of the complexes of (TPP)MnX and showed large scatter in the data. This would imply that solvent bonding is not the dominant factor in determining $E_{1/2}$ and that another correlation is needed. One such correlation that works reasonably well is that of $E_{1/2}$ vs. solvent dielectric constant.

Figure 4 plots and half-wave potentials of the metal-centered reactions of the N_3^- and ClO_4^- salts of $[(TPP)Mn^{III}]^+$ vs. the dielectric constant of the solvent. In those solvents having a donor number less than 25, the potentials of $(TPP)MnClO_4$

(30) V. Gutmann, "The Donor-Acceptor Approach to Molecular Interactions", Plenum Press, New York, 1978.
(31) K. M. Kadish, L. A. Bottomley, S. Kelly, D. Schaeper, and L. R. Shiue, *Bioelectrochem. Bioenerg.*, **8**, 213 (1981).
(32) J. F. Kirner, C. A. Reed, and W. R. Scheidt, *J. Am. Chem. Soc.*, **99**, 2557 (1977).
(33) W. R. Scheidt and C. A. Reed, *J. Am. Chem. Soc.*, **97**, 3247 (1975).
(34) L. K. Hanson and B. M. Hoffman, *J. Am. Chem. Soc.*, **102**, 4602 (1980).
(35) V. Gutmann, *Struct. Bonding (Berlin)*, **15**, 141 (1973).
(36) W. R. Scheidt, J. F. Kirner, and C. A. Reed, *J. Am. Chem. Soc.*, **99**, 1093 (1977).
(37) H. A. O. Hill, A. J. Macfarlane, and R. J. P. Williams, *J. Chem. Soc. A*, 1704 (1979).
(38) F. A. Walker, *J. Magn. Reson.*, **15**, 201 (1974).
(39) G. P. Fulton and G. N. LaMar, *J. Am. Chem. Soc.*, **98**, 2119 (1976).
(40) G. P. Fulton and G. N. LaMar, *J. Am. Chem. Soc.*, 2124 (1976).
(41) R. H. Felton, G. S. Owen, D. Dolphin, and J. Fajer, *J. Am. Chem. Soc.*, **93**, 6332 (1971).
(42) M. A. Phillipi, E. T. Shimoura, and H. M. Goff, *Inorg. Chem.*, **20**, 1322 (1981).
(43) P. Gans, J. C. Marchon, and C. A. Reed, *Nouv. J. Chim.*, **5**, 201 (1981).
(44) Values of (free ligand) were obtained from the mass balance equations for $(TPP)MnClO_4$ and ligand and the stability constants determined spectroscopically. The program used for these calculations has been previously described.[45]
(45) D. J. Leggett, *Talanta*, **24**, 535 (1975).

Table III. Half-Wave Potentials (V) vs. SCE of the First Porphyrin Ring Reduction for (TPP)MnX in Selected Solvents

solvent	DN	dielec const	AN[a]	counterion, X					
				ClO_4^-	I^-	SCN^-	Br^-	Cl^-	N_3^-
$EtCl_2$	0.0	10.7		−1.51	−1.52		−1.51	−1.52	−1.52
PhCN	11.9	25.2	15.5	−1.34	−1.34	−1.57	−1.37	−1.48	−1.48
CH_3CN	14.1	37.5	19.3			−1.46	−1.47	−1.47	−1.47
PrCN	16.6	20.3		−1.37	−1.37	−1.49		−1.48	−1.47
THF	20.0	7.6	8.0	−1.33	−1.32	−1.33	−1.33	−1.34	−1.46
DMF	26.6	38.3	16.0	−1.29	−1.30	−1.30	−1.31	−1.32	−1.31
DMA	27.8	37.8	13.6	−1.23	−1.22	−1.22	−1.22		−1.24
Me_2SO	29.8	46.4	19.3	−1.28	−1.28	−1.27	−1.27	−1.27	−1.27
py	33.1	12.0	14.2	−1.30	−1.30	−1.31	−1.31	−1.31	−1.30

[a] Acceptor number.

and $(TPP)MnN_3$ are well separated, and two nearly parallel lines can be drawn through the points. The potential for the metal-centered reaction shifts positively as the dielectric constant of the solvent increases. Such behavior is expected upon formation of a charged species from a neutral species. An earlier postulate that the halide remains associated in nonbonding solvents[11] is also consistent with the shift of potential shown in Figure 4 and can be accounted for by formation of negatively charged $[(TPP)MnX]^-$ upon reduction of (TPP)MnX.

In the more strongly coordinating solvents DMA, DMF, Me_2SO, and pyridine (DN > 25), reduction of (TPP)MnX is independent of counterion and does not fit on a line as shown in Figure 4. Spectroscopic studies of $(TPP)MnClO_4$ and (TPP)MnCl in solutions containing 0.1 M TBAP show that both Me_2SO and pyridine will displace the counterion on (TPP)MnX and form six-coordinate complexes with two solvent molecules acting as the fifth and sixth axial ligands. The invariance of reduction potentials for (TPP)MnX in pyridine and Me_2SO as seen in Table I also strongly indicates the complete replacement of X^- by a solvent molecule before electroreduction. In this case the electroreduction is best described by eq 3.

$$[(TPP)Mn^{III}S_2]^+X^- \overset{e^-}{\rightleftharpoons} [(TPP)Mn^{II}S] + X^- + S \quad (3)$$

So that the changeover from (TPP)MnX to $(TPP)Mn(py)_2^+$ as reactant could be monitored, half-wave potentials were measured for the reduction of $(TPP)MnClO_4$, (TPP)MnCl, and $(TPP)MnN_3$ in $EtCl_2$/pyridine mixtures. This is illustrated in Figure 5, which plots the reduction potentials of (TPP)MnX in $EtCl_2$ (0.1 M TBAP)/pyridine mixtures with different concentrations of pyridine. In the absence of pyridine (neat $EtCl_2$) $(TPP)MnClO_4$ is reduced at −0.17 V. Both (TPP)MnCl and $(TPP)MnN_3$ have more negative reduction potentials due to stabilization of Mn(III) by the counterion and are reduced at −0.26 and −0.31 V, respectively. As seen in Figure 5 the addition of pyridine has little effect upon the Mn(III)/Mn(II) couple of $(TPP)MnN_3$ but causes a cathodic shift in potentials for reduction of $(TPP)MnClO_4$ and (TPP)MnCl. The slope of this shift is 53 mV/decadic increase in pyridine concentration. This slope agrees well with the theoretical slope for the loss of one ligand upon reduction[46] and has been shown by spectrophotometric investigations (reported later in this paper) to be due to the reduction of the six-coordinate $(TPP)Mn(py)_2^+$, which yields the five-coordinate reduced product (TPP)Mn(py).[32]

At pyridine concentrations greater than 0.1 M, both $(TPP)MnClO_4$ and (TPP)MnCl solutions have the same potential for each pyridine concentrations, suggesting the same species exists in both solutions. Constancy of the $(TPP)MnN_3$ solution half-wave potentials with increase in pyridine concentration

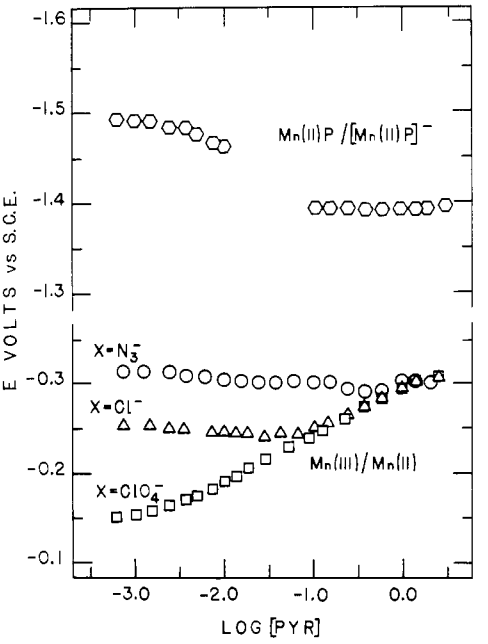

Figure 5. Plot of half-wave potential vs. the concentration of added pyridine for the first two reductions of (TPP)MnX (X = ClO_4^-, Cl^-, N_3^-) in $EtCl_2$ solutions containing 0.1 M TBAP.

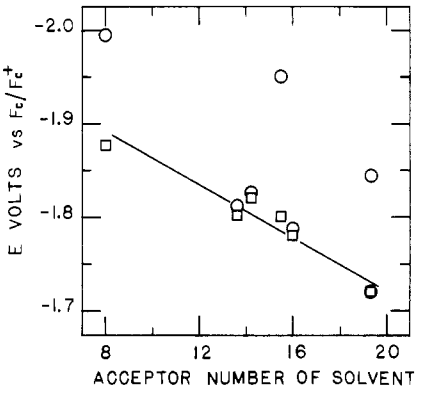

Figure 6. Plot of half-wave potential vs. the acceptor number of that solvent for the first porphyrin ring reduction of $(TPP)MnClO_4$ (□) and $(TPP)MnN_3$ (○) in seven nonaqueous solvents.

from log (py) = −3.0 to log (py) = 0.0 shows that N_3^- is a sufficiently strong counterion to prevent complete pyridine association up to concentrations well above 1.0 M, and suggests that the mono(pyridine) adduct $(TPP)Mn(py)N_3$ will predominate even at high pyridine concentrations. Similar results are obtained upon addition of Me_2SO to $EtCl_2$ solutions of (TPP)MnX (X = ClO_4^-, Cl^-, N_3^-).

Porphyrin Ring Reactions. The first porphyrin ring reduction is observable in all solvents except $MeNO_2$, where the poor cathodic solvent range precluded its observation. In

(46) I. M. Kolthoff and J. J. Lingane, "Polarography", Vol. I, 2nd ed., Interscience, New York, 1952, p 66.

Table IV. Half-Wave Potentials (V) vs. SCE of the First Porphyrin Ring Oxidation for (TPP)MnX in Selected Solvents

			counterion, X					
solvent	DN	dielec const	ClO_4^-	I^-	SCN^-	Br^-	Cl^-	N_3^-
$MeCl_2$	0.0	8.9	+1.19	+1.19	+1.19	+1.19	+1.14	+1.18
$EtCl_2$	0.0	10.7	+1.21	+1.21	+1.21	+1.20	+1.17	+1.19
PhCN	11.9	25.2	+1.25	+1.26	+1.24	+1.25	+1.24	+1.24
CH_3CN	14.1	37.5	+1.25	+1.25	+1.24	+1.25		+1.24
PrCN	16.6	20.3	+1.28	+1.29	+1.28	+1.28		

$MeCl_2$, and acetone, the reduction was not reversible at a Pt-button electrode or a HMDE. Table III reports the half-wave potentials of the first ring reduction in the other seven solvents studied. In contrast to the metal-centered reaction, the dielectric constant is not a good solvent parameter for the porphyrin ring reactions. As the acceptor number of the solvent increases, there is a fairly linear stabilization of the reduced ring species over the neutral ring species. This behavior, which is shown in Figure 6, reflects the ability of the solvent to accommodate the increased electron density on the ring and is not without precedent.[35] The presence of interactions between the porphyrin π ring and solvent could explain this behavior. Crystallographic structural determination of (TPP)Mn^{II} has shown weak π bonding between toluene solvate molecules and the porphyrin ring.[36] Hill et al.[37] have studied weak π complexes with manganese porphyrins, and other metalloporphyrin systems, and have shown similar interactions.[38-40]

The effect of changing the coordination of the porphyrin upon the ring reduction can be seen in Table III and Figure 7. The first porphyrin ring reduction occurs at −1.51 V vs. SCE in $EtCl_2$ and is independent of counterion within experimental error. The addition of pyridine to solutions of (TPP)MnX causes the disappearance of the original couple and the simultaneous appearance of a new couple at −1.39 V vs. SCE in $EtCl_2$/pyridine mixtures. (Note that this potential differs from that of −1.31 V in Table III due to differences in liquid-junction potentials between the two solvent systems.) This new couple predominates completely at pyridine concentrations greater than 0.1 M and is also independent of counterion, as seen for the case of ClO_4^-, Cl^-, and N_3^- in Figure 5. A similar reduction mechanism is observed when Me_2SO, DMF, or DMA is added to $EtCl_2$ solutions containing (TPP)MnX. This mechanism also occurs if the initial solvent is THF, or $MeCl_2$, and reflects the greater ability of DMA, Me_2SO, and pyridine to stabilize the generated porphyrin radical.

The first ring reduction of (TPP)MnX in the solvents benzonitrile and butyronitrile show a counterion dependence. Indeed, the range of $E_{1/2}$ in benzonitrile extends over 200 mV, rivaling the counterion dependence found for the metal-centered reaction. It is interesting to note that there is a simple division into "weak" and "strong" counterions. The "weak" counterions (ClO_4^-, I^-, and sometimes Br^-) have the same potential for ring reduction, suggesting the counterion is sufficiently displaced from the site of reduction as to exert no stabilizing effect. However, the "strong" counterions destabilize reduction by ~0.1 V and have nearly the same effect, with the exception of SCN in benzonitrile. The division between "weak" and "strong" counterions suggests that the "weaker" counterions have a higher probability for dissociation from (TPP)Mn^{II} than the "stronger" counterions within the time scale of the experiment. The species whose potential is more negative reflect a counterion more tightly bound to (TPP)Mn^{II}. It should be mentioned that the solubility of these compounds is small and very near the concentration range used in this experiment. The solubility in MeCN is greatest for the ClO_4^- complex and least for the N_3^- complex and decreases in the order of $E_{1/2}$ found for the metal-centered reactions,

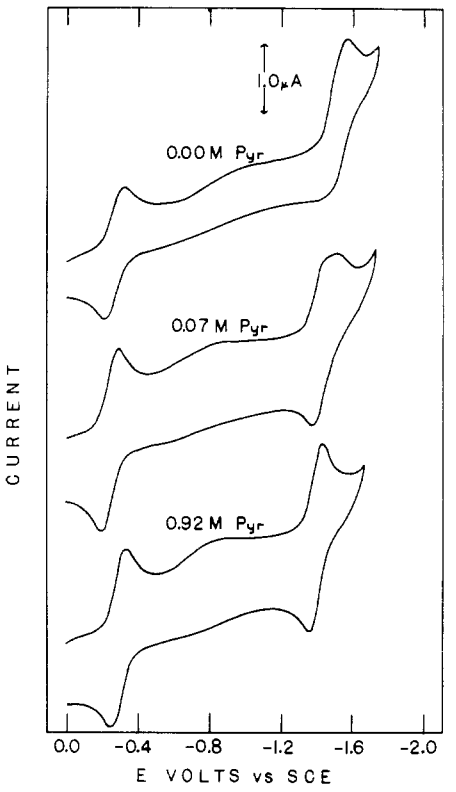

Figure 7. Cyclic voltammograms of (TPP)$MnClO_4$ in $EtCl_2$ solution containing 0.1 M TBAP and various concentrations of pyridine at a scan rate of 200 mV/s.

with the exception of that for the SCN^- complex. The low solubility of these complexes may emphasize the effects of axial interactions in these solvents. A similar explanation would account for the destabilization of the first ring reduction of (TPP)MnN_3 in THF by about 0.1 V relative to that of the other (TPP)MnX complexes.

Oxidation of (TPP)MnX. Half-wave potentials for oxidation of (TPP)MnX are shown in Table IV for six counterions and the five solvents showing reversible ring oxidations at a Pt electrode. These values are uncorrected for liquid-junction potential but appear to vary little as a function of solvent or counterion. This is similar to results obtained for oxidation of (TPP)FeX.

As seen from this table, these five solvents show a linear stabilization of the lower oxidation state over the higher oxidation state with increasing donor number. Stabilization through σ interactions with the solvent would predict the opposite behavior,[30] and the trend provides further support for the importance of interaction between the porphyrin π ring and solvent. Unfortunately, the effects of solvation by strong donor molecules such as Me_2SO and pyridine upon ring oxidation were not observable, as addition of these solvents to (TPP)MnX in weakly bonding solvents such as $EtCl_2$ destroyed the reversiblility of these reactions.

Unlike the controversy surrounding the site of oxidation in (TPP)FeX,[41-43] there appears to be little doubt that, with Mn complexes in nonaqueous media, the reaction site involves the

π-ring system. Thus the overall reaction can be represented as

$$(TPP)Mn^{III}X \rightleftarrows [(TPP)Mn^{III}X]^+ + e^- \quad (4)$$

Constancy of $E_{1/2}$ with changes in X lends support to the assignment of π cation radical formation.

Formation Constants for Axial Ligation to Mn(III) and Mn(II). In previous evaluations of metalloporphyrin half-wave potentials, it was noted that potentials for the reaction M(III) $\rightleftarrows$ M(II) were directly related to the ratio of stability constants for ligand or solvent addition to the central metal in each oxidation state. This effect is most dramatic for reactions of Fe(III) and Co(II) porphyrin complexes, where large differences exist between the M(II) and M(III) form of the metal. In the case of (TPP)$CoClO_4$ and (TPP)$FeClO_4$ reductions, an increase in solvent donor number yields a large cathodic shift of potential due to the increased preference of solvent for the higher oxidation state.[31] In contrast, reduction of (TPP)FeX, where X = N_3^-, Cl^-, or Br^-, shows an anodic shift of potential with increase in donor number, indicating that the reduced form is preferentially stabilized by solvent.[20]

For both the iron and cobalt complexes a large amount of information exists on the stability constants for the oxidized and reduced forms of the complex, and correlation with half-wave potentials is straightforward. This is not the case with manganese porphyrins, where less information exists on ligand addition thermodynamics for either Mn(III) or Mn(II) complexes.[11,15] The reason for this lack of data is that very small spectral changes are known to occur upon complexation of the stable Mn(III) species and determinations of log β_1 or log β_2 are difficult by routine methodologies. Further problems are also presented with Mn(II) complexes in that this oxidation state is extremely unstable at room temperature and facile oxidation or side reactions may occur in the presence of trace oxygen or ligand impurities. For this reason it was necessary to directly determine stability constants for ligand addition under the same experimental conditions as in our electrochemical experiments. This was done with a combination of electrochemical and spectrochemical techniques. The ligands investigated were Me_2SO and pyridine, both of which were also used as solvents. For comparison, complexation with imidazole was also investigated.

Me_2SO, pyridine, or imidazole was added to solutions of (TPP)$MnClO_4$ in $EtCl_2$, and cyclic voltammograms were recorded at various concentrations of added ligand. From the cyclic voltammograms the half-wave potential, $E_{1/2}$, as well as the anodic and cathodic peak potentials, E_{pa} and E_{pc}, was measured and plotted vs. the log of free ligand concentration.[44] Half-wave potentials for imidazole and pyridine solutions shifted cathodically at greater than 1:1 ligand:porphyrin ratios, whereas a higher concentration of Me_2SO was required to induce a cathodic shift. The slopes of these plots ranged from −0.053 to −0.060 V/tenfold increase in ligand concentration. The peak separation, $E_{pa} - E_{pc}$, indicated that the Mn(III)/Mn(II) couple remained quasi-reversible during addition of pyridine or Me_2SO, but irreversible electron transfer began to dominate the solutions containing greater than 0.04 M imidazole. For the purpose of this paper the electrochemical investigations are limited to solutions that are less than 0.04 M in imidazole, where reversibility occurred.

In an earlier study[11] plots of $E_{1/2}$ vs. log C_L were used to simultaneously determine the stoichiometry and stability constants for ligand binding to the oxidized and reduced porphyrin. On the basis of these observations, and the constancy of $E_{1/2}$ for ligand concentrations less than 0.001 M, one of the following two electrode reactions may be postulated:

$$(TPP)MnClO_4 + e^- \rightleftarrows (TPP)Mn + ClO_4^- \quad (5a)$$

$$(TPP)Mn(L)ClO_4 + e^- \rightleftarrows (TPP)Mn(L) + ClO_4^- \quad (5b)$$

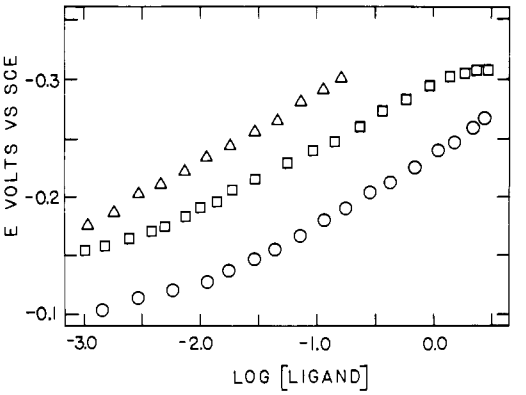

Figure 8. Plot of half-wave potentials for the reduction of [(TPP)$Mn(L)_2]^+$ in $EtCl_2$, 0.1 M TBAP, where L = imidazole (△), pyridine (□), and Me_2SO (○).

At higher ligand concentrations, additions of Me_2SO, pyridine, or imidazole to (TPP)$MnClO_4$ solutions resulted in a cathodic shift of the Mn(III) reduction potentials by −0.053 to −0.060 V/decade change of ligand concentration as shown in Figure 8. Both the direction and magnitude of the shift are those predicted theoretically[46] for the stabilization of Mn(III) relative to Mn(II) and the loss of one ligand concomitant with electroreduction.

On the basis of this shift of potential, electroreduction for these concentrations may be represented by either of the following plausible reactions:

$$(TPP)Mn(L)ClO_4 + e^- \rightleftarrows (TPP)Mn + L + ClO_4^- \quad (6a)$$

$$(TPP)Mn(L)_2{}^+ClO_4^- + e^- \rightleftarrows (TPP)Mn(L) + L + ClO_4^- \quad (6b)$$

In reaction 6a the counterion is shown as associated to Mn(III) while in reaction 6b it is necessarily shown as dissociated. No proof exists for the former assignment in $EtCl_2$ solutions containing 0.1 M TBAP.

All four electrode reactions described by reactions 5 and 6 are reasonable. However, by purely electrochemical methods, differentiation of the exact electrode reaction and elucidation of the individual stability constants are not possible. In this case, an understanding of the electrochemical reactions hinges upon independent identification of the trivalent metalloporphyrin complexes stable in solution. Analysis of the spectral data offers the best chance of success.

In order to do this, we recorded the electronic absorption of $EtCl_2$ solution containing 10^{-5} M (TPP)$MnClO_4$, 0.10 M TBAP, and increasing concentrations of ligand, L. The spectrum of (TPP)$MnClO_4$ in the absence of ligand has the split Soret band characteristic of trivalent manganese porphyrins; these bands have been designated as bands V and VI in previous studies.[7] The positions and relative intensities of bands V and VI agree well with published values for (TPP)$MnClO_4$ in toluene.[27] Addition of each ligand shifted the bands toward lower wavelengths and increased the absorbance ratio of band V over band VI. These two effects were most evident when the ligand was Me_2SO. Concentrations of each ligand were increased until no further changes were observed in the visible spectra.

The best fit of SQUAD to the experimental data was observed when (TPP)$Mn(L)ClO_4$ and (TPP)$Mn(L)_2{}^+ClO_4^-$ were included in the equilibrium model. This was true for all three ligands. All other models tested led to either nonconvergence or significantly inferior fits to the experimental data. The output from SQUAD includes the molar absorptivities, at all wavelengths considered, of each species present in solution. These data are presented in Figure 9.

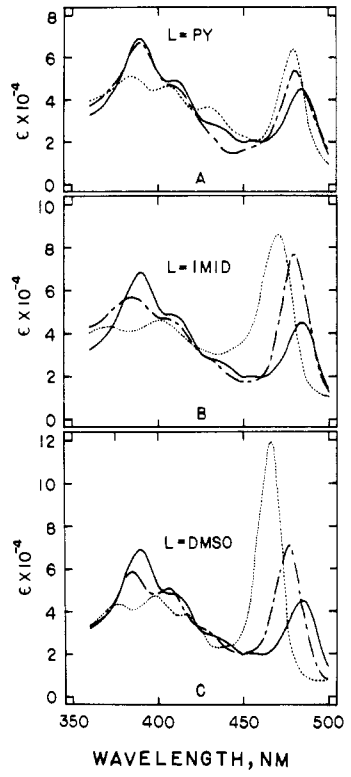

Figure 9. Computer-generated molar absorptivities from 360 to 500 nm for $(TPP)MnClO_4$ (solid lines), $[(TPP)Mn(L)]^+$ (dashed lines), and $[(TPP)Mn(L)_2]^+$ (dotted lines) in $EtCl_2$ solutions containing 0.1 M TBAP, where L = pyridine (A), imidazole (B), and Me_2SO (C).

Scheme I

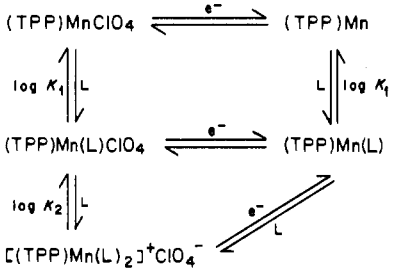

As seen in Figure 9 there is a systematic change in the absorbance spectra between $(TPP)MnClO_4$, $(TPP)Mn(L)ClO_4$ and $(TPP)Mn(L)_2^+ClO_4^-$. In contrast, previous workers have observed little change in spectra between five- and six-coordinate manganese porphyrins.[7,14,47,48] However, the cases cited always involve a strongly binding counterion (such as Cl^-, N_3^-) as one of the axial ligands. We also observed that, when X is a strongly binding counterion (such as Br^-, Cl^-, or N_3^-) and L is Me_2SO, pyridine, or imidazole, the spectrum of (TPP)MnX is not easily distinguished from that of (TPP)Mn(L)X.[49] However, independent of counterion there is a significant change between the spectra of (TPP)Mn(L)X and $(TPP)Mn(L)_2^+X^-$. Since most earlier studies of ligand addition have started with (TPP)MnCl and not $(TPP)MnClO_4$ as the reactant, one can see how the spectral change associated with the formation of $(TPP)Mn(L)_2^+X^-$ could be mistaken for the formation of (TPP)Mn(L)X. Thus, the unusually low estimates of K_1 for the species (TPP)Mn(py)Cl in chloroform (25 °C) determined by Hambright[50] could in fact be estimates of β_2 for the species $(TPP)Mn(py)_2^+Cl^-$.

(47) K. Moffat, R. S. Loe, and B. M. Hoffman, *J. Mol. Biol.*, **104**, 669 (1976).
(48) B. M. Hoffman and Q. H. Gibson, *Biochemistry*, **15**, 3405 (1976).
(49) S. Kelly and K. M. Kadish, unpublished results.

Table V. Stability Constants for Axial Ligation of $(TPP)Mn^{III}ClO_4$ and $(TPP)Mn^{II}$ in 1,2-Dichloroethane (0.1 M TBAP)[a]

complex	metal oxidn state	const	imidazole	pyridine	Me_2SO
$(TPP)MnClO_4$	III	$\log K_1$	4.35 ± 0.04	4.08 ± 0.04	3.49 ± 0.01
		$\log \beta_2$	7.45 ± 0.04	6.99 ± 0.07	5.74 ± 0.02
(TPP)Mn	II	$\log K_1$	4.12 ± 0.2	4.55 ± 0.2	4.38 ± 0.2

[a] Error estimates for the Mn(III) complexes were provided by SQUAD. Estimates for the Mn(II) complexes are based on a maximum uncertainty of ±10 mV in the potential measurements.

Combined Electron Transfer and Ligand Reaction Mechanism. On the basis of the electrochemical and electronic absorption data, the overall electron transfer and ligand reaction mechanism, shown in Scheme I, is postulated. A list of stability constants is given in Table V.

The reactant in the absence of ligand is $(TPP)MnClO_4$, which undergoes a quasi-reversible electron transfer in $EtCl_2$ to yield (TPP)Mn. Addition of a stoichiometric amount of ligand shifts the equilibrium toward the formation of $(TPP)Mn(L)(ClO_4)$. When this species is reduced, the product is always (TPP)Mn(L). Further addition of ligand forms $(TPP)Mn(L)_2^+ClO_4^-$, which is reduced at the electrode to from (TPP)Mn(L). This change of coordination number upon reduction is responsible for the cathodic shift of the metal-centered reaction with increasing ligand concentration, as seen in Figure 8.

The stability constants given in Table V for $(TPP)Mn(L)ClO_4$ and $(TPP)Mn(L)_2ClO_4$ formation are taken directly from the spectroscopic data. On the other hand, log β_1 for (TPP)Mn(L) formation was calculated from the spectroscopically determined log β_2 for $(TPP)Mn(L)_2^+ClO_4^-$ formation and the Nerstian slopes of Figure 8. This assumes the predominance of reaction 6b in this region. On the basis of the spectroscopic evidence, there is no doubt that this is the prevailing electrode reaction.

It is interesting to note that comparable values of log K_1 are obtained for Mn(III) and Mn(II) when the axial ligand is imidazole or pyridine. The existence of comparable stability constants for the mono(imidazole) or mono(pyridine) complexes of Mn(III) and Mn(II) implies that there should be little shift in potential for the

$$(TPP)Mn(L)ClO_4 \overset{e^-}{\rightleftharpoons} (TPP)Mn(L)$$

couple in relation to the

$$(TPP)MnClO_4 \overset{e^-}{\rightleftharpoons} (TPP)Mn$$

couple. Indeed, this is what is observed experimentally. In contrast, comparison of the stability constants for Me_2SO addition suggests that an anodic shift of approximately 50 mV should be observed; when a stoichiometric amount of Me_2SO is added to the solution, an anodic shift of 45 mV is observed, consistent with the values of log K_1 for Mn(III) and Mn(II).

For both the mono- and bis(ligand) complexes of Mn(III), there is a decrease in the complex stability in going from imidazole to pyridine to Me_2SO. The formation constants with Me_2SO are significantly smaller and reflect the weaker interaction between the Mn(III) center and oxygen donors relative to nitrogen donors. Of the nitrogenous bases, imidazole forms a stronger complex, which is reasonable when two points are considered. Axially bound imidazole experiences less steric interaction with the porphyrin π electrons than pyridine, and

(50) P. C. Hambright, *Chem. Commun.*, 470 (1967).

its higher pK_a (6.6 vs. 5.3) would suggest a stronger σ bond relative to pyridine.

In a previous work, Boucher[7] proposed that the relative stability of Mn(III) porphyrin complexes could be predicted by the relative positions of band V in the electronic absorption spectra. Specifically, the complex that was most stable would have the peak maxima of band V occurring at the highest energy. Applying this rule to the ligands in Table V, one would predict pyridine to form the weakest complex (band V occurs at 480 nm), followed by imidazole (472 nm) and then by Me_2SO, which forms the strongest complex (464 nm). One can see that the validity of this rule is in question when applied to ligands containing different donor atoms, although it may be valid for ligands containing the same donor atom.

In contrast to the Mn(III) complexes, the Mn(II) complexes are all of roughly equal stability. The higher electron density on Mn(II) reduces the importance of σ donation from the axial ligand. Mn(II) has been shown to lie significantly farther out of the porphyrin plane and provides much less steric interactions with axial ligands than does Mn(III). In addition, the Mn d orbitals, which are involved in π bonding to the porphyrin in Mn(III), are avilable to interact with the axial ligand. Although Mn(II) complexes with pyridine and imidazole are thought to involve pure σ bonding,[34] π bonding may contribute to the Me_2SO complex and account for its higher stability relative to that of the Mn(III) complex.

It should be pointed out that the measured $\log K_1 = 4.55$, for pyridine addition to Mn(II), is almost 2 orders of magnitude larger than that previously reported for addition of pyridine to Mn(II) when the starting complex was (TPP)MnCl ($\log K_1 = 2.70$).[11] This increase in stability constant is consistent with the lack of binding of a ClO_4^- anion to Mn(II), as was postulated when the starting material contained a Cl^- counterion. Likewise, the difference between the values of Mn(III) ligand addition when the starting materials were (TPP)$MnClO_4$ ($\log K_1 = 4.08$) and (TPP)MnCl ($\log K_1 = 1.10$)[11] is also consistent with the difference in binding strengths between (TPP)Mn^+ and the halide or the perchlorate counterion. No comparable values have been published for addition of Me_2SO or imidazole to (TPP)MnCl.

In summary, we have observed that manganese porphyrins are greatly influenced by the strong interaction between the porphyrin π ring and the Mn(III) center. The influence of counterions and solvent upon metal-centered reductions is greatly reduced relative to iron and cobalt porphyrins.[31] For solvents of low coordinating ability (DN < 25), the counterion is associated, while more strongly coordinating solvents displace the counterion, in qualitative agreement with other studies. The coordinating ability of Mn(III) toward σ donors is nearly equal to that of Mn(II) and explains the relatively small potential dependence upon solvents of widely varying donicities.

Finally, the work has provided the first measured stepwise stability constants for the addition of axial ligands to a Mn(III) porphyrin in nonaqueous media. Moreover, the data analysis has revealed the spectrum of an intermediate five-coordinate Mn(III) porphyrin complex with axial ligands. When combined with electrochemical measurements of stability constant ratios, values of $\log K_1$ may also be obtained for addition of the same ligands to Mn(II). The values measured for addition of Me_2SO, pyridine, and imidazole to (TPP)Mn (generated from (TPP)$MnClO_4$) are consistent with those previously presented in the literature.

Acknowledgment. The support of the National Science Foundation (Grant No. CHE-7921536) is gratefully acknowledged. We also acknowledge the help of Dr. David Leggett in analyzing the spectrophotometric data via SQUAD.

Registry No. (TPP)$MnClO_4$, 67161-73-3; (TPP)MnI, 55290-33-0; (TPP)MnSCN, 82613-97-6; (TPP)MnBr, 55290-32-9; (TPP)MnCl, 32195-55-4; (TPP)MnN_3, 56413-47-9; CH_2Cl_2, 75-09-2; $ClCH_2CH_2Cl$, 107-06-2; CH_3NO_2, 75-52-5; PhCN, 100-47-0; CH_3CN, 75-05-8; PrCN, 107-12-0; $(CH_3)_2CO$, 67-64-1; THF, 109-99-9; DMF, 68-12-2; DMA, 127-19-5; Me_2SO, 67-68-5; py, 110-86-1; [(TPP)$Mn(Im)_2]^+$, 82613-98-7; [(TPP)$Mn(py)_2]^+$, 82613-99-8; [(TPP)$Mn(Me_2SO)_2]^+$, 82614-00-4; (TPP)Mn, 31004-82-7.

Contribution from the Istituto Chimica Generale, University of Pisa, 56100 Pisa, Italy

Transition-Metal-Catalyzed Oxidation of Carbon Monoxide by Dichlorine To Produce Phosgene

FAUSTO CALDERAZZO* and DANIELA BELLI DELL'AMICO

Received December 29, 1981

Halometal carbonyls of gold, palladium, and platinum catalyze the formation of $COCl_2$ from carbon monoxide and dichlorine at atmospheric pressure and room temperature under exclusion of light. Semiquantitative data show that the catalytic efficiency in this homogeneous process is Au > Pd > Pt. Attack at the carbonyl carbon of soluble halo–carbonyl complexes by coordinated chloride or by dichlorine to give unstable M–C(O)–Cl groupings is believed to be operative in these processes.

Although the formation of $COCl_2$ from carbon monoxide and dichlorine is a highly exothermic reaction,[1] the kinetics of the reaction are such that thermal activation on active coal or light promotion is required.[2] Although trisubstituted phosphine oxides have been used[3] for the catalytic combination of carbon monoxide at superatmospheric pressure with dichlorine at room temperature, we are not aware of any report on transition-metal-catalyzed formation of phosgene at room temperature.

We had already noted[4,5] that phosgene is frequently the only observable product of the reduction of some late-transition-metal halides (Au(III), Pt(IV)) by carbon monoxide. Thus,

(1) "Kirk-Orthmer Encyclopedia of Chemical Technology", 3rd ed.; Wiley: New York, 1978; Vol. 4, p 777. Davies, J. V.; Pritchard, H. O. *J. Chem. Thermodyn.* **1972**, *4*, 23–29.
(2) "Gmelins Handbuch der Anorganischen Chemie"; Springer-Verlag: West Berlin, 1972; Carbon Compounds, Part C2, p 145.
(3) Masaki, M.; Kakeya, N.; Fujimura, S. *J. Org. Chem.* **1979**, *44*, 3573–3574.
(4) Belli Dell'Amico, D.; Calderazzo, F. *Gazz. Chim. Ital.* **1973**, *103*, 1099–1104; **1979**, *109*, 99.
(5) Belli Dell'Amico, D.; Calderazzo, F.; Marchetti, F. *J. Chem. Soc., Dalton Trans.* **1976**, 1829–1831.

0020-1669/82/1321-3639$01.25/0